

E. Ruzanski*

Colorado State University, Fort Collins, CO

Y. Wang

Colorado State University, Fort Collins, CO

V. Chandrasekar

Colorado State University, Fort Collins, CO

1. INTRODUCTION

This paper describes an operational system implementation and performance evaluation of the Dynamic and Adaptive Radar Tracking of Storms (DARTS) nowcasting system within the Collaborative and Adaptive Sensing of the Atmosphere (CASA) X-band radar network (Brotzge et al. 2005). The nowcasting algorithm and operational nowcasting system architecture are described. Verification of the real-time operation and performance of DARTS is presented using data collected from a severe weather event during the CASA Integrative Project 1 (IP1) experiment in 2008.

2. THE DARTS ALGORITHM

There currently exist three general classes of extrapolative nowcasting algorithms. The first approach involves identifying the spatially distributed motion field by maximizing the cross-correlation over subgrids in two successive radar images (Chornoboy et al. 1994; Rinehart and Garvey 1978). The second approach, referred to as "centroid tracking" (Austin and Bellon 1982), defines storm cells using certain characteristic parameters. These cell objects are identified and tracked using various heuristic or optimization algorithms. The third class, to which the DARTS algorithm belongs, contains algorithms which involve estimating deterministic physical model parameters (Zawadzki and Germann 2002).

Several algorithms have been developed with various enhanced features based on these three fundamental approaches. The Growth and Decay Storm Tracker (GDST) algorithm employs an elliptical spatial filter to smooth the radar images and enable tracking systematic growth and decay propagations of the large-scale component in storms (Wolfson et al. 1999). The Storm Cell Identification and Tracking (SCIT) algorithm combines both approaches (Johnson et al. 1998). Another commonly used procedure, Thunderstorm Identification, Tracking, Analysis, and Nowcasting (TITAN), is based on the identification of storm position, size, and mergers and splits (Dixon and Weiner 1993).

* *Corresponding author address:* Evan Ruzanski, Department of Electrical and Computer Engineering, Colorado State University, Fort Collins, CO 80523; e-mail: ruzanski@engr.colostate.edu.

The DARTS algorithm is built upon the general flow equation modified for nowcasting, given by,

$$\frac{\partial}{\partial t} F(x, y, t) = -U(x, y) \frac{\partial}{\partial x} F(x, y, t) - V(x, y) \frac{\partial}{\partial y} F(x, y, t) + S(x, y, t) \quad (1)$$

where $F(x, y, t)$ is the scalar field of radar observations, $U(x, y)$ is the x-axis motion velocity field, $V(x, y)$ is the y-axis motion velocity field, and $S(x, y, t)$ can be interpreted as the additive dynamic mechanisms, such as growth and decay. Eq. (1) is then represented in discrete form as a linear model and solved in the Fourier space using Linear Least-Squares Estimation. Thus, the novelties of this method are that the model is able to separate the storm motion from local and additive growth and decay mechanisms and is developed in the spectral domain, such that the various scales of both storm and motion field can be controlled by the choice of Fourier coefficients. The DARTS algorithm is "dynamic" in the sense it is built upon this fluid dynamics-based equation and is "adaptive" in the sense the tracking scale can be selected by choosing the number of leading Fourier coefficients.

When compared with the cross-correlation method, the DARTS algorithm also has several other advantages. It is global in the sense that the estimated motion field can be constructed over the whole spatial region where radar images are rendered avoiding the necessity to employ local block windows thus reducing computational load and mitigating aperture effects. The smoothness of the estimated motion field is controlled by the selection of fewer leading Fourier coefficients.

The next section describes the operational system architecture in which the DARTS nowcasting algorithm was implemented and evaluated during the CASA IP1 experiment in 2008.

2. OPERATIONAL NOWCASTING SYSTEM ARCHITECTURE

The DARTS algorithm was implemented within the CASA X-band radar network to provide end-users with real-time predicted reflectivity images for lead times up to 10 minutes. The overall system diagram is shown in Figure 1.

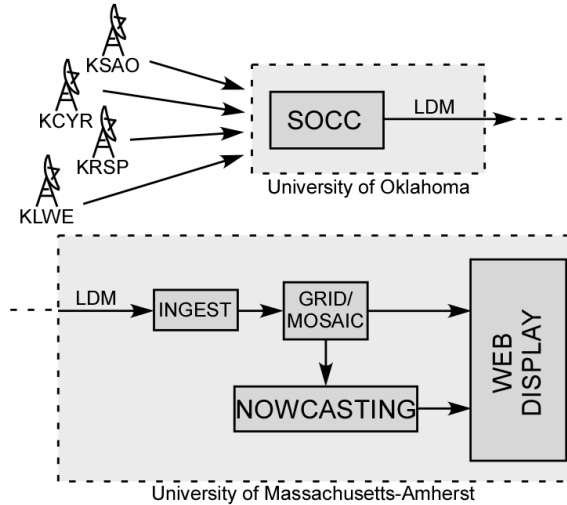


Figure 1. Operational CASA nowcasting system architecture.

Attenuation correction and clutter removal algorithms are employed at each of the 4 CASA radar nodes at Chickasha (KSAO), Rush Springs (KRSP), Cyril (KCYR), and Lawton, Oklahoma (KLWE). The System Operations Control Center (SOCC, SOCC-CASA 2009) located at the University of Oklahoma at Lawton, OK, receives the radar node data, performs conversion to Network Common Data Format (NetCDF), and sends the data to the University of Massachusetts at Amherst via a Local Data Manager (LDM, LDM 2009). After the radar data files are suitably synchronized by the ingester, the individual radar data files are gridded and mosaiced. These gridded and mosaiced data files serve as input to the DARTS nowcasting module, which provides the predicted reflectivity images to the end-user via an Internet-based display. The system diagram of the operational DARTS software module is shown in Figure 2.

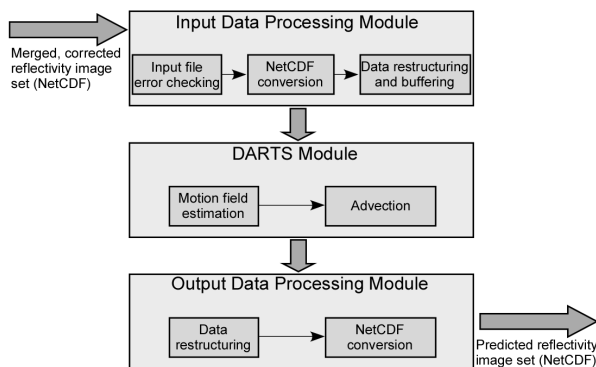


Figure 2. Operational DARTS software module.

The operational performance of the DARTS nowcasting module is described in the following section.

3. PERFORMANCE RESULTS

Radar reflectivity data collected from the CASA radar network from a storm event occurring November 5, 2008, was used as input to the DARTS and GDST nowcasting algorithms. The storm exhibited shear profiles of 60 knots combined with strong heating in downslope westerly flow in the wake of the dry line. These conditions lead to the development of severe thunderstorms including supercells initially near the dry line/cold front intersection. The storm moved quickly to the northeast at an average velocity of about 45 mph. While a tornado warning was issued, no tornadoes developed, although there were reports of hail up to 1.75 inches in diameter and winds gusts of 64 mph. More damage reports were issued for this storm case than any other since beginning CASA radar data collection in 2006.

The data collected from this event was gridded to 0.5 km average spatial resolution at a height of 1 km above ground level (AGL). The settings for each nowcasting algorithm were selected to give the best performance using results from prior heuristic experiments. An example 10-minute prediction using the DARTS algorithm is compared to the current-time and 10-minute observed images is shown in Figure 3.

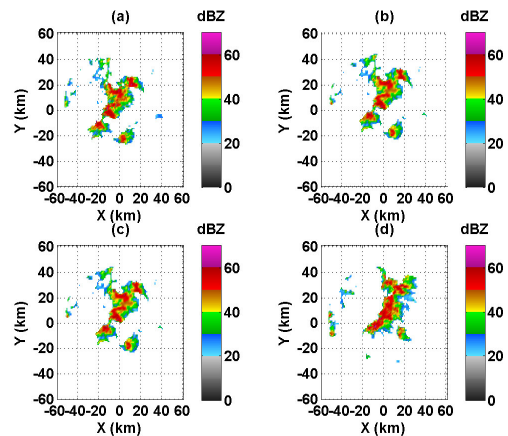


Figure 3. Observed and predicted reflectivity images from the Nov. 5, 2008, CASA IP1 storm event: (a) current observed image; (b),(c) 10-minute predicted reflectivity images generated using the DARTS algorithm; (d) 10-minute observation.

The performance of the DARTS algorithm in real-time was compared to the GDST algorithm (off-line) using Critical Success Index (CSI), Probability of Detection (POD), and False Alarm Ratio (FAR) skills scores (Wilks 2005). CSI, POD, and FAR are defined, respectively, as,

$$CSI = \frac{hits}{hits + misses + false\ alarms} \quad (2)$$

$$\text{POD} = \frac{\text{hits}}{\text{hits} + \text{misses}} \quad (3)$$

$$\text{FAR} = \frac{\text{false alarms}}{\text{hits} + \text{false alarms}} \quad (4)$$

where a “hit” is defined as an active (or inactive) pixel within a square sub-area in the predicted image centered on a corresponding active (or inactive) pixel in the observed image. The term “active” refers to a pixel value that is equal to or greater than a predefined threshold level. Likewise, an “inactive” pixel is one whose value is less than a predefined threshold value. A “false alarm” is defined as the condition of presenting an active pixel within a square sub-area in the predicted image centered on an inactive pixel in the observed image. A “miss” is defined as the condition of presenting no active pixels within a square sub-area in the predicted image centered on an active pixel in the observed image. A 2 X 2 km scoring area size and threshold of 25 dBZ was used in the scoring procedure. For DARTS, a history time of 10 minutes was used for motion field estimation.

Figures 4, 5, and 6 show the CSI, POD, and FAR scores, respectively, for lead times up to 10 minutes for both DARTS and GDST. These figures show DARTS slightly outperforms the GDST algorithm in tracking performance. On average, DARTS shows an average improvement of 5.6% in CSI scores with similar improvement is seen in the POD and FAR scores.

An important feature of the DARTS algorithm is the significant reduction in runtime versus GDST. This point is critical when considering application in the CASA integrated weather radar network with scan rates as low as 1 minute. Preliminary studies have shown motion field generation took approximately 1.8 seconds to complete, on average, using the DARTS algorithm on a Linux platform. Using a comparable GDST implementation, average motion field generation took approximately 20 seconds. This represents a significant time reduction factor when using DARTS versus GDST nowcasting algorithms.

4. CONCLUSIONS AND FUTURE WORK

The DARTS nowcasting algorithm has been described. An operational system diagram of the nowcasting system integrated within the CASA radar network was also presented. The DARTS algorithm was comparatively evaluated against the GDST algorithm using data collected during the Nov. 5 severe storm event during the 2008 CASA IP1 experiment. The results show that the operational DARTS algorithm was approximately 5.6% more accurate than the GDST algorithm for this data set using CSI, POD, and FAR skill scores as performance measures. Additionally, the DARTS algorithm was shown to run about 10 times faster than GDST on average for this data set.

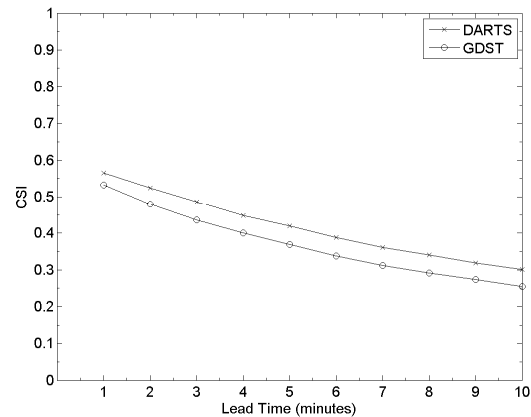


Figure 4. CSI score comparison between the DARTS (operational) and GDST (off-line) algorithms for the Nov. 5, 2008, CASA IP1 storm event.

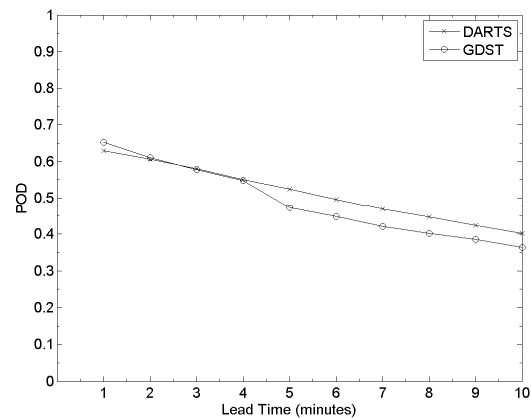


Figure 5. POD score comparison between the DARTS (operational) and GDST (off-line) algorithms for the Nov. 5, 2008, CASA IP1 storm event.

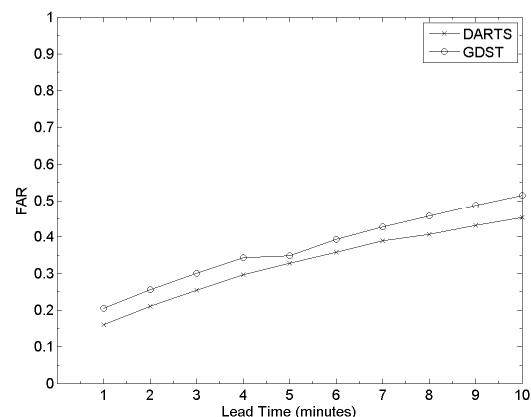


Figure 6. FAR score comparison between the DARTS (operational) and GDST (off-line) algorithms for the Nov. 5, 2008, CASA IP1 storm event.

The DARTS algorithm is currently operating in the CASA network. Future work includes the addition of real-time scoring to monitor nowcasting performance operationally with the CASA system. It is also planned to use predicted reflectivity images in the closed-loop to "steer" the radar nodes to better monitor areas where severe weather will likely be present. Future work also includes analyzing and enhancing the DARTS model to better understand the physical characteristics of severe convective weather and improve nowcasting performance of such.

Acknowledgement. This work was supported by the Engineering Research Center Program of the National Science Foundation under NSF award number 0313747 and the NSF-LEAD ITR program.

6. REFERENCES

- Austin, G.L., and A. Bellon, 1982: Very short-range forecasting of precipitation by the objective extrapolation of radar and satellite data, *Nowcasting*, A.K. Browning, ed. Academic Press, 177-190.
- Brotzge, J., and Coauthors, 2005: CASA's First Test Bed: Integrative Project #1, Preprints, *32nd Conf. Radar Meteor.*, Amer. Meteor. Soc., Albuquerque, NM.
- CASA Home Page, cited 2009: Center for Collaborative Adaptive Sensing of the Atmosphere. [Available online at <http://www.casa.umass.edu>.]
- Chornoboy, E.S., and Coauthors, 1994: Automated storm tracking for terminal air traffic control, *Lincoln Laboratory Journal*, **7**: 427-448.
- Dixon, M., and G. Weiner, 1993: TITAN: thunderstorm identification, tracking, analysis, and nowcasting – a radar-based methodology, *J. Oceanic and Atmos. Technol.*, **10**: 785-797.
- Johnson, J.T., and Coauthors, 1998: The storm cell identification and tracking algorithm: an enhanced WSR-88D algorithm, *Weather and Forecasting*, **13**:263-276.
- Rinehart, R.E., and E.T. Garvey, 1978: Three-dimensional storm motion detection by conventional weather radar, *Nature*, **273**: 287-289.
- SOCC-CASA, cited 2009: IP1 Integrative Project 1. [Available online at <http://socc.caps.ou.edu>.]
- Unidata Local Data Manager (LDM), cited 2009: Local Data Manager (LDM). [Available online at <http://www.unidata.ucar.edu/software/ldm>.]
- Wilks, D.S., 2005: Statistical Methods in the Atmospheric Sciences, 2e. Academic Press, 263-265.
- Wolfson, M.M., and Coauthors, 1999: The growth and decay storm tracker, Preprints, *8th Conf. on Aviation, Range, and Aerospace Meteor.*, Dallas, TX, Amer. Meteor. Soc., 58-62.
- Zawadzki, I., and U. Germann, 2002: Scale-Dependence of the Predictability of Precipitation from Continental Radar Images. Part I: Description of Methodology, *Mon. Wea. Rev.*, **130**: 2859-2873.